JOURNAL OF MATERIALS SCIENCE **36** (2001) 2581–2587

Sintering and crystallisation of a P_2O_5-added Li_2O-ZrO_2-SiO_2 glass powder system

A. P. NOVAES DE OLIVEIRA
Center of Ceramic Technology, Rua Gen. Lauro Sodré, 300-P.O.Box 3247, Bairro Comerciário, 88802-330, Criciuma (SC) Brazil

T. MANFREDINI
Department of Chemistry, Faculty of Engineering, University of Modena, Via Campi 183, 41100 Modena, Italy

Sintering and crystallisation of a 11.5 wt % Li_2O, 22.8 wt % ZrO_2, 65.7 wt % SiO_2 glass powder with P_2O_5 added were investigated. By means of thermal shrinkage measurements, sintering was found to start at about 650°C and was completed in a very short temperature interval ($\Delta T \approx 100$°C) in less than 30 min. Crystallisation took place just after completion of densification and was almost completed at about 900°C in 20 min. Secondary porosity prevailed over the primary porosity during the crystallisation stage. The glass powder compacts first crystallised into lithium metasilicate (Li_2SiO_3) and/or zircon ($ZrSiO_4$) and tridymite (SiO_2) which transformed and/or grew into lithium disilicate ($Li_2Si_2O_5$), zircon and tridymite after the crystallisation process was essentially complete, so that, a crystallinity degree between 52.4 ± 2.0 and 68.5 ± 3.2 wt % was obtained. P_2O_5 doping little affected the densification. However, adding P_2O_5 remarkably enhanced the zircon and tridymite crystallisation while delaying the Li_2SiO_3 to $Li_2Si_2O_5$ transformation. The microstructure is characterised by fine crystals uniformly distributed arbitrarily oriented throughout the residual glass phase.

1. Introduction

Glass-ceramic materials are polycrystalline solids containing a residual glassy phase, made by controlled crystallisation of particular formulated glasses [1, 2] such that glass articles are obtained by the usual means of glass technology and their subsequent crystallisation. However, this technology requires heavy investment and can be justified only for large volume production, while production of glass-ceramics by sintering of glass powders can be performed using the ordinary equipment of a ceramic factory and is especially suitable for the manufacture of small quantities of articles with complicated shapes [2]. This method of combining the powder particles to form a bulk material essentially follows the principles of conventional sintered ceramic technology. The difference lies in that starting powder is a glass and the sintering and crystallisation processes occur in the one firing cycle [3] since, the nature of the particle surface results in a predominance of surface crystallisation. In this case, small amounts of P_2O_5 typically within the limits of 0.5 to 3 wt % can aid control of the sintering/crystallisation behaviour as has been reported [4, 5]. The densified body can eventually crystallise throughout, resulting in a fully dense, sintered glass-ceramic. However, residual porosity will always be present and so high density sintered bodies can be excluded.

Thus, in this work the sintering and crystallisation of a 11.5 wt % Li_2O, 22.8 wt % ZrO_2, 65.7 wt % SiO_2 glass powder doped with P_2O_5 were investigated, by means of differential thermal analysis (DTA), X-ray diffraction at room (XRD) and at elevated temperatures (HT-XRD), scanning electron microscopy (SEM) and thermal shrinkage measurements.

2. Experimental procedure

The nominal compositions of the glasses studied are shown in Table I. P_2O_5 was added to a 11.5 wt % Li_2O, 22.8 wt % ZrO_2, 65.7 wt % SiO_2 glass composition. Well-mixed powders containing the appropriate amounts of Li_2CO_3, $ZrSiO_4$, SiO_2 and $NH_4H_2PO_4$ were used as raw materials. Subsequently, the batches were placed in a Pt crucible and melted at 1500°C for 7 h in a electrically heated furnace. The melts were cast into deionized water to provide frits for milling. Then, the glass frits were dried and dry-crushed in alumina ball-mills for 2 h as well as sieved to yield a powder particle size <45 μm. The crushed glass powders were then milled for 48 h in aluminous porcelain mills containing alumina balls, ethanol and 1 wt % of polyvinyl alcohol (PVA) as binder. The resulting slurries were dried to a humidity content of about 5.5% and the average particle size was found to be 2 μm by using a laser scattering particle size analyser (Model Analysette 22, Fritsch). The glass powders were then uniaxially pressed by means of an automatic hydraulic

TABLE I Nominal compositions of glasses studied

Glass Compositions	Constituents (wt %)	
	11.5 Li_2O-22.8ZrO_2-65.7SiO_2	P_2O_5
GCZ	100.0	-
GCZP15	98.5	1.5
GCZP30	97.0	3.0

press at 40 MPa (green density about 1.45 g cm^{-3}) in a 13 mm diameter steel mold and the resulting green samples were prefired for 1 h at 500°C to burn off the binder. A decrease in green density <1% was observed after binder burnout. The temperature for the binder burnout was determined by thermogravimetric analysis (TGA - Model STA 409, Netzsch) in alumina (100 mg samples) crucibles at a heating rate of 10°C min^{-1} in air. After binder burnout samples were isothermally sintered in a laboratory electric furnace (±5°C) in air for appropriate time intervals (30–120 min) at $T = 800$°C, 850 °C and 900°C. After completion of sintering, samples were air-quenched to room temperature. No cracks were visually observed. Linear shrinkage's of each sample and glass composition at each temperature and time were measured. Green and sintered samples were measured dimensionally with a screw micrometer. Thermal shrinkage's were also measured by means of a hot stage microscope-HSM (trade name MISURA) at 10°C min^{-1} in air. In this case, the apparatus consisted of a horizontal tube furnace with specimen carriage, a light source to illuminate the field of view fully and uniformly, an electronic video camera and a special optical lens designed to obtain maximum resolution (10 μm). Drop profile (dimensional changes) and images can be printed out when the HSM analysis have been completed by a special computer programme. The temperature is read with a 2°C resolution and measured by means of a Pt/Pt-Rh thermo-element placed directly under the sample and digitalized. The crystallisation temperatures of the glass powders were measured by differential thermal analysis (DTA) in air at a heating rate of 10°C min^{-1} using about 30 mg of powdered samples. A DSC Model 404 high-temperature Netzsch thermoanalyzer was used with an empty Pt crucible as reference material. To investigate the amorphous nature of the as-quenched glasses and the crystalline phases of the sintered samples, powdered samples were analysed with a Philips PW 3710 computer-assisted X-ray (Cu K α) powder diffractometer (XRD). X-ray diffraction at elevated temperatures (HT-XRD) was also employed. The crystallinity of the sintered and crystallised samples was also determined by applying the Chung's method [6] using α-Al_2O_3 as reference material. The densities for the green and sintered samples were measured by the Archimedes principle with mercury immersion at 20°C. Sintered samples were cut and their cross sections were mounted in epoxy resin, then the surfaces were ground smooth, polished with 1 μm alumina paste and etched (2% HF, 25 s). Subsequently, all the samples were coated with a thin Pd-Au film for scanning electron microscopy (SEM) observations (Model Philips XL-40).

3. Results and discussion

3.1. Sintering

Viscous flow dominates for amorphous materials [7], such that a small and a narrow particle-size distribution is fundamental for obtaining a high sintered density [8]. However, during sintering there is competition between sintering and crystallisation and it is generally considered [9] that a high final density can only be achieved if sintering proceeds almost to completion before the crystallisation starts and causes the viscosity of the material to increase to such an extent that continued densification via viscous flow becomes impossible. In fact, densification can be limited to the crystallisation stage since secondary porosity usually appears, especially when the crystallinity and size of crystals increases, according to the studies of Rabinovich [10] regarding to coordierite glass-ceramics produced by sintering.

The thermal linear shrinkage curves of the studied glasses obtained by hot stage microscope measurements are shown in Fig. 1. From the figure it can be seen that densification starts for all the glass compositions at about 650°C and is completed in a very short temperature interval ($\Delta T \approx 100$°C) and it is constant, up to about 850°C. However, it increases slightly from GCZ to GCZP15 glass compositions respectively. Between 850 and 950°C a slight increase in volume is observed since crystallisation starts very soon after the completion of sintering. Above 950°C a new and strong increase in volume caused by the growth and/or melting of the crystalline phases take place. In fact, as shown in Fig. 2 which refers to DTA curves of the glass powders, the same effects as mentioned above can be observed: endothermal inflections at about 596°C, 602°C and 614°C related to the glass transition, exothermal peaks having maxima at about 865°C, 865°C and 851°C which are correlated with the crystallisation processes and endothermal effects having maxima at about 982°C, 967°C and 959°C related to the melting of crystalline phases for the GCZ, GCZP15 and GCZP30 glass compositions respectively.

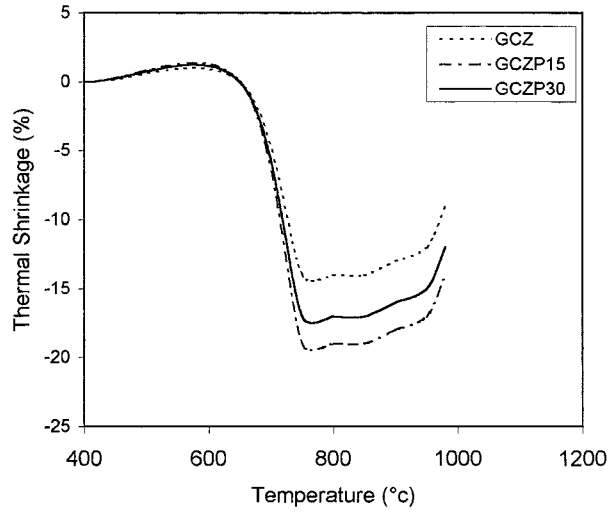

Figure 1 Thermal linear shrinkage of the glass powders studied, compacted at 40 MPa (heating rate 10°C min^{-1}).

The effect of sintering time and temperature on the densification of the studied glasses are shown in Figs 3–5. The green density is about 1.45 g/cm^3 (the lower end of the ordinate axis) and the examination of

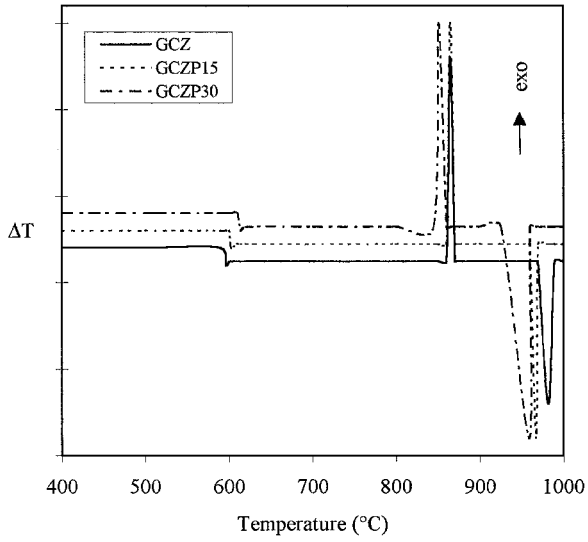

Figure 2 DTA curves of the glass powders studied (heating rate 10° min^{-1}).

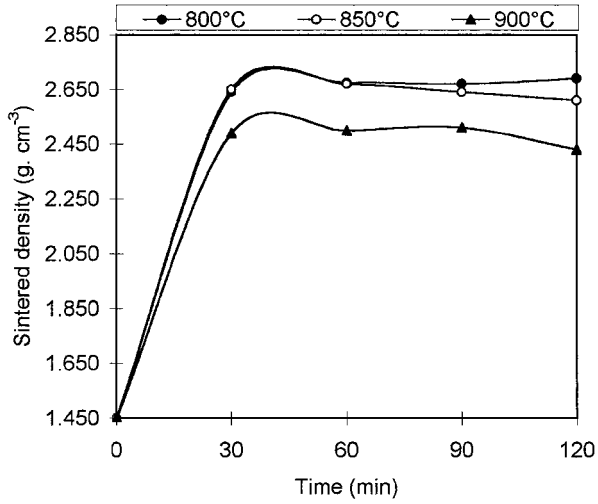

Figure 3 Sintered density of glass powder compacts (GCZ) versus time for sintering temperatures of 800°C, 850°C and 900°C.

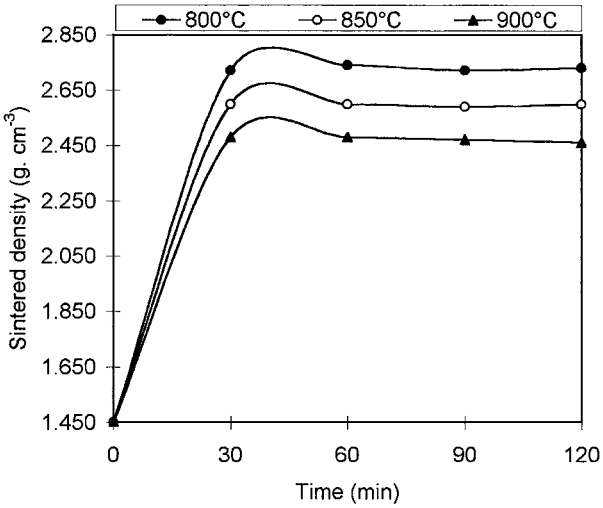

Figure 4 Sintered density of glass powder compacts (GCZP15) versus time for sintering temperatures of 800°C, 850°C and 900°C.

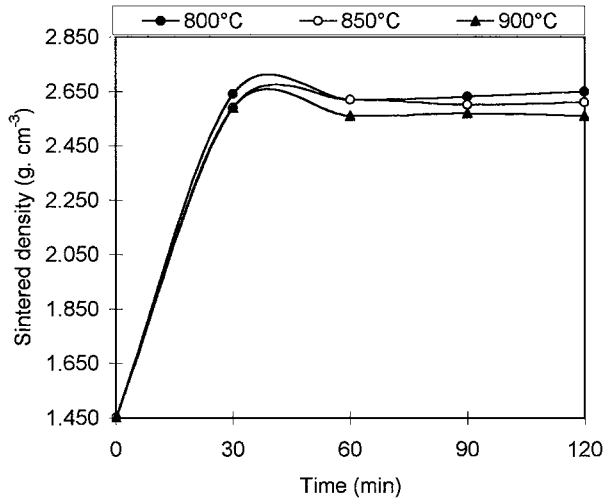

Figure 5 Sintered density of glass powder compacts (GCZP30) versus time for sintering temperatures of 800°C, 850°C and 900°C.

the figures show that the sintered density for all the glasses increases as the temperature decreases from 900°C to 800°C and rapidly becomes almost constant as the heating time increases. This indicates that most of the densification takes place in a very narrow range of heating time (<30 min) in good agreement with the thermal linear shrinkage measurements. The decrease of the sintered density as the temperature increases is related to the crystallisation processes which will be indicated and discussed later. In addition, the sintering temperature did not have a strong effect on the sintered density in the sintering time intervals studied.

3.2. Crystallisation

Figs 6–8 show the XRD patterns related to the as-quenched glasses and those sintered at 800°C, 850°C and 900°C for 60 min respectively for each glass composition. From Fig. 6 which is related to the glass composition GCZ it can be seen that the reflections associated with the sample sintered at 800°C for 60 min (Fig. 6b) were assigned to the crystalline phases of lithium metasilicate (Li_2SiO_3), file JCPDS n° 29-828. On the other hand, in the samples sintered at 850°C (Fig. 6c) and 900°C (Fig. 6d) for 60 min respectively, the reflections related to the crystalline phase of

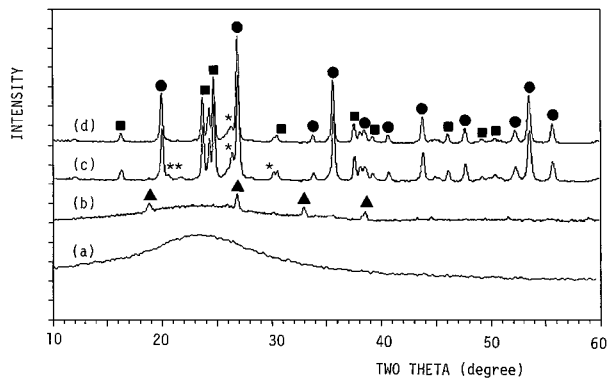

Figure 6 Powder XRD patterns of samples (GCZ): (a) as-quenched glass; (b) sintered at 800°C for 60 min, (c) sintered at 850°C for 60 min and (d) sintered at 900°C for 60 min. ▲ - Li_2SiO_3; ■ - $Li_2S_2O_5$; ● - $ZrSiO_4$ and * - tridymite.

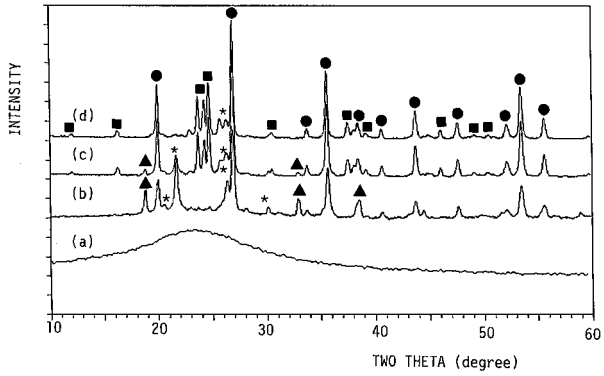

Figure 7 Powder XRD patterns of samples (GCZP15): (a) as-quenched glass; (b) sintered at 800°C for 60 min, (c) sintered at 850°C for 60 min and (d) sintered at 900°C for 60 min. ▲ - Li_2SiO_3; ■ - $Li_2S_2O_5$; ● - $ZrSiO_4$ and * - tridymite.

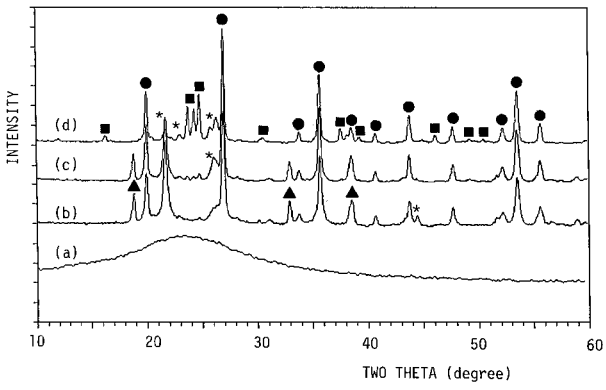

Figure 8 Powder XRD patterns of samples (GCZP30): (a) as-quenched glass; (b) sintered at 800°C for 60 min, (c) sintered at 850°C for 60 min and (d) sintered at 900°C for 60 min. ▲ - Li_2SiO_3; ■ - $Li_2S_2O_5$; ● - $ZrSiO_4$ and * - tridymite.

lithium metasilicate disappeared, the crystalline phases of lithium disilicate ($Li_2Si_2O_5$), files JCPDS n° 24-651, 30-767, zircon ($ZrSiO_4$), file JCPDS n° 6-266 and tridymite (SiO_2), files JCPDS n° 12-708, 14-260, evolving. However, the reflections associated with the X-ray pattern of the sintered sample at 900°C increased in intensity, indicating that the crystallisation processes are almost completed, according to the DTA curve. The XRD pattern shown in Fig. 6a regarding to the as-quenched glass, demonstrates its amorphous nature since it is characteristic of the glassy state. These results were also obtained in previous work of ours [11] for the same glass system but for a different composition. Fig. 7 shows the XRD patterns of glass composition GCZP15. In this case, the crystalline phases developed during the heat-treatments of sintering are the same that those of glass composition GCZ at 900°C, except that they were formed very soon at 800°C (Fig. 7b) and increased in intensity as the temperature was increased. Meanwhile, tridymite was seen to increases with respect to the glass composition GCZ and by increasing the sintering temperature up to 850°C (Fig. 7c). At 900°C (Fig. 7d) the tridymite amounts was decreased. This decrease can be associated with the mechanism of lithium disilicate and zircon formation as was suggested in an our previous work [11]. On the other hand, the XRD patterns related to the glass composition GCZP30 (Fig. 8) show that except for the lithium disilicate all the other crystalline

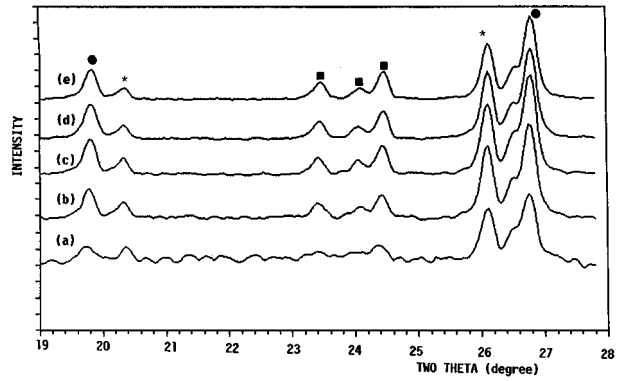

Figure 9 Powder XRD at 900°C after (a) 5 min; (b) 10 min; (c) 20 min; (d) 40 min and (e) 60 min (heating rate 100°C min^{-1}). ■- $Li_2S_2O_5$; ● - $ZrSiO_4$ and * - tridymite.

phases were formed at 800°C (Fig. 8b). Tridymite was formed in high amounts initially, decreasing later with an increasing sintering temperature.

From these results, it can be seen, that doping of 3 wt % of P_2O_5 lowered the crystallisation temperature from 865°C to 851°C according to DTA curves, favouring and accelerating the formation of zircon. Note that, also in this case, the XRD patterns regarding to the as-quenched glasses GCZP15 (Fig. 7a) and GCZP30 (Fig. 8a) demonstrate their amorphous nature.

Considering that the crystallisation is almost completed at 900°C, as shown above, and to verify the time effect on the crystallisation, the glass powders were subjected to X-ray diffraction at elevated temperatures (HT- XRD). In this case, the glass powders were heated up to 900°C at a heating rate of 100°C min^{-1} and then XRD patterns of the isothermally powdered samples were recorded at 5, 10, 20, 40 and 60 min respectively as shown in Fig. 9 related to the glass composition GCZ as an example. According to the HT-XRD patterns of Fig. 9, a detectable amount of the same crystalline phases observed in the XRD of Figs 6d, 7d and 8d is formed. It appears that the crystallisation processes are almost completed after 20 min (Fig. 9c) since for higher crystallisation times the peak diffraction intensities are almost the same.

3.3. Sintering and crystallisation relation

SEM observations on etched surfaces of partially and fully sintered powder compacts provide a good insight into the processes accuring during densification and crystallisation. Consequently, Fig. 10a and b regarding glass composition GCZ show the microstructures of samples heated at 800°C and 850°C for 60 min respectively. Fig. 10a shows that almost all of the fine scale porosity is eliminated in 60 min at 800°C, so that the pore size and the pore fraction represent the degree of densification. In fact, according to Figs 1 and 3, at 800°C densification is already completed and it is the maximum. This is also valid for glass compositions GCZP15 and GCZP30. However, there is clear evidence of crystallisation which appears to have nucleated at the boundaries of the original glass powder particles, in agreement with the XRD of the Fig. 6b. As evidenced in Fig. 10b showing the sample sintered for 60 min at 850°C, although the crystalline phases, mainly zircon

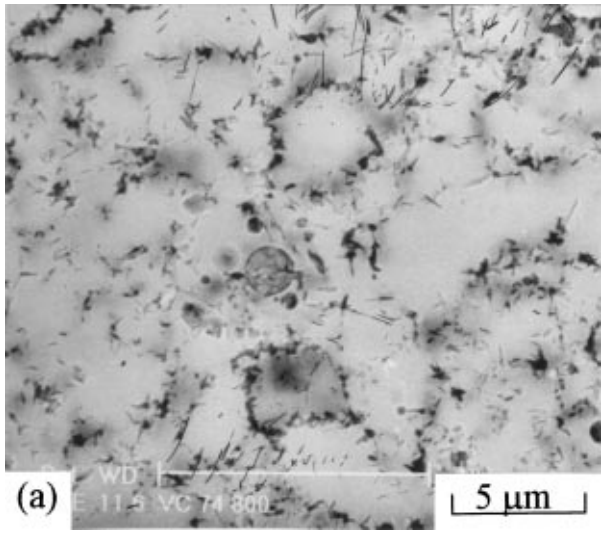

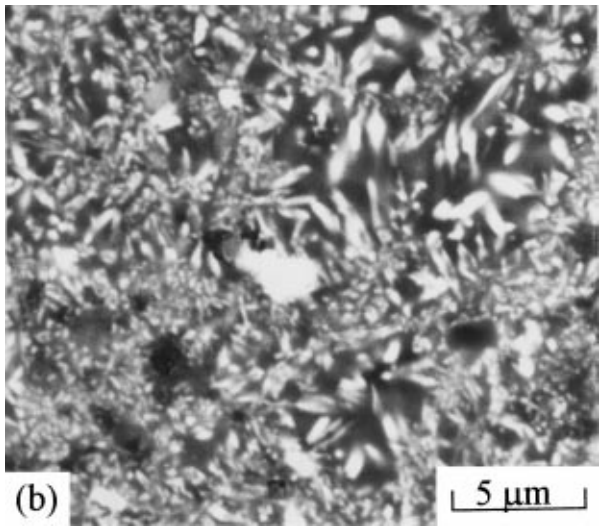

Figure 10 SEM micrographs of glass powder compacts (GCZ) sintered at (a) 800°C and (b) 850°C for 60 min, respectively.

and lithium disilicate have been formed, the crystallisation process is not finished, since some regions containing original glass powder particles (glassy phase) are visible, confirming the XRD pattern of Fig. 6c and also those of Figs 7c and 8c. In the samples sintered for 60 min at 900°C (Fig. 11a–c) no isolated regions containing glassy phases are observed, which indicates that the crystallisation process is almost finished, in agreement with the XRD patterns of Figs 6d, 7d and 8d. On the other hand, by comparing the micrographs related to samples sintered at 850°C and 900°C with those sintered at 800°C, in this case, represented by Fig. 10a, it can be seen that secondary porosity appears and is higher when the crystallisation is completed. In this case, the number and size of the secondary pores are affected by the amount of crystals and not by their size, since for samples sintered at 900°C for 30 min and 120 min (Fig. 12a and b) related to the glass composition GCZ there is no clear evidence of crystal growth and the porosity representing the densification is about the same over time as was shown in Figs 3–5. This evidence well explains the decrease of the sintered density with the increases of temperature. The decrease of densification above 950°C (Fig. 1) can be associated with an increase of the secondary porosity caused by crystal growth and also by their melting according to DTA curves. Fig. 12c shows the morphology of the crystals of a sample (GCZ) sintered at 950°C for 30 min where crystal growth can be evidenced by comparing with Fig. 12a. Although the crystallisation process has been already completed at 900°C after 60 min, the microstructure consists of fine crystals distributed uniformly and arbitrarily throughout a residual glass phase.

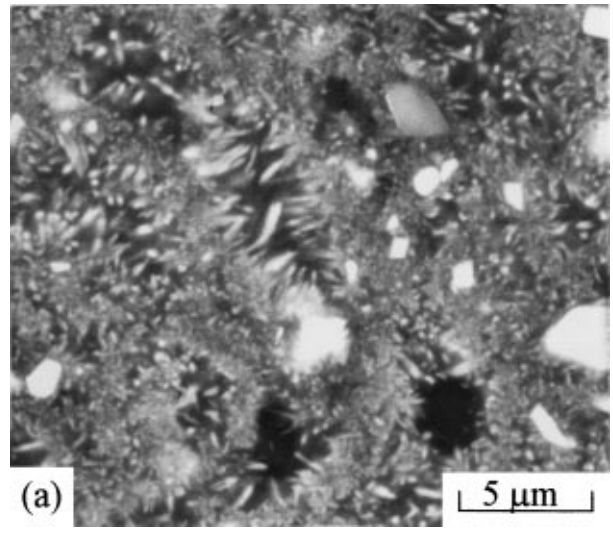

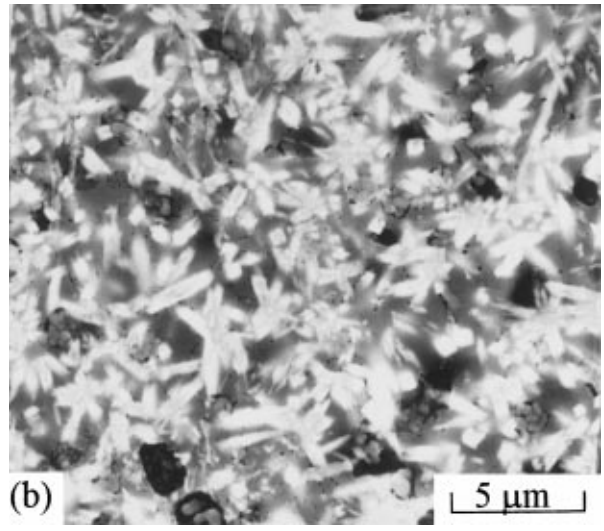

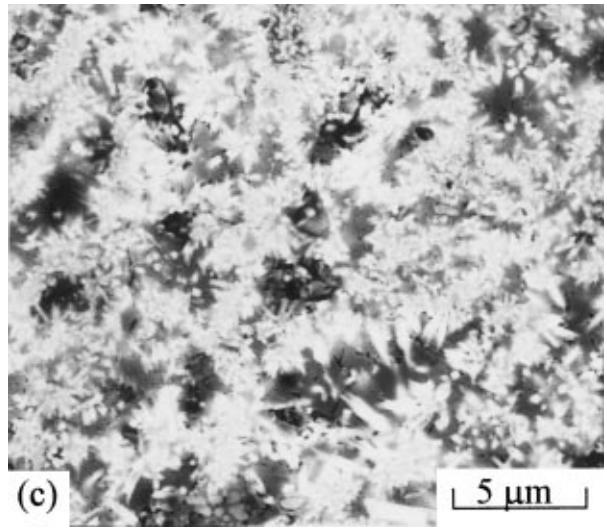

Figure 11 SEM micrographs of glass powder compacts sintered at 900°C for 60 min. (a) GCZ, (b) GCZP15 and (c) GCZP30.

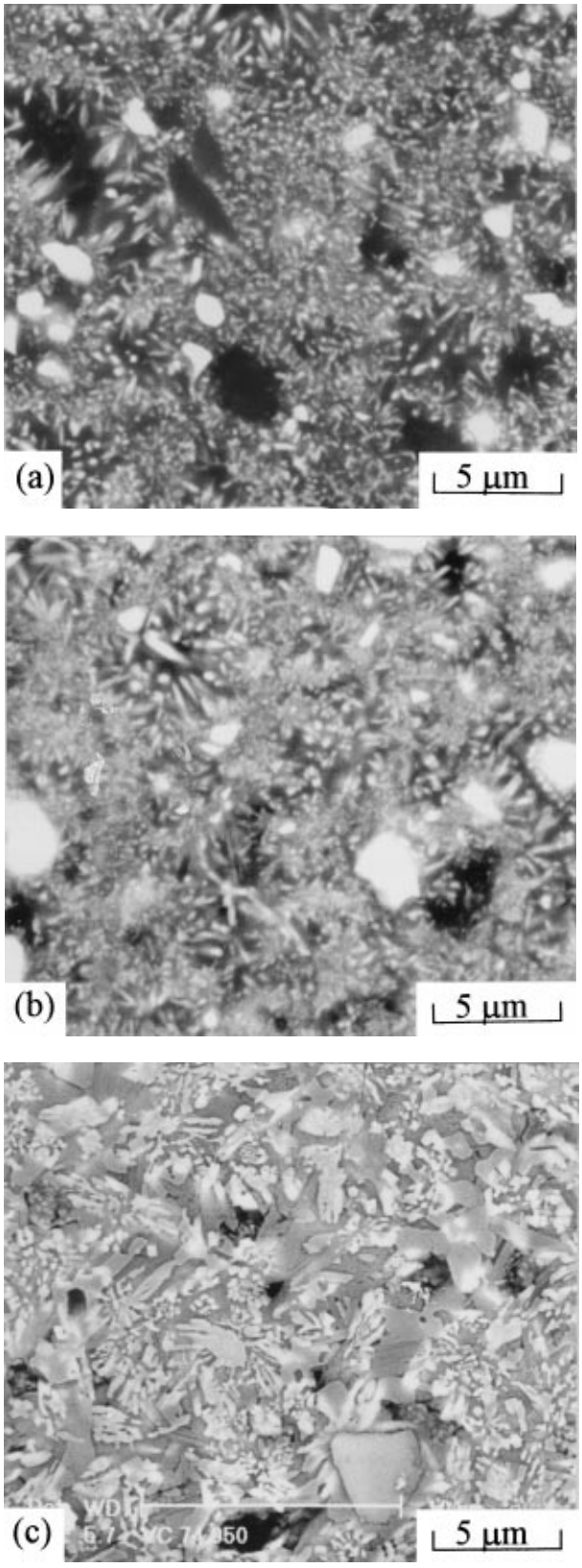

Figure 12 SEM micrographs of glass powder compacts (GCZ) sintered at (a) 900°C for 30 min, (b) 900°C for 120 min and (c) 950°C for 30 min.

The crystal sizes of glass composition GCZP15 seems to be higher and of a lower number. In fact, the crystallinity of samples sintered at 900°C for 60 min was found to be 68.5 ± 3.2, 56.3 ± 2.5 and 52.4 ± 2.0 wt % for the glass compositions GCZ, GCZP15 and GCZP30 respectively. So, the degree of crystallinity is higher for glass compositions GCZ and GCZP15 and lower for glass composition GCZP30. With these additional data we can make some considerations to explain the densification behaviour during crystallisation.

The slight but higher degree of densification of glass composition GCZP15 with respect to the other ones, according to Fig. 1, can be attributed to the P_2O_5 addition effects on crystallisation. According to the XRD and micrographs of the P_2O_5 glasses, zircon seens to be the favoured crystalline phase. In fact, incorporation of 1 mol % P_2O_5 in $Li_2O.\ 2SiO_2$ glass affect the viscosity by only a small amount compared with the large effect on nucleation rate [3, 12]. This indicates that the main effect of P_2O_5 is to reduce the free energy for nucleation (ΔG^*) rather than the free energy for diffusion (ΔG_D). In this work the P_2O_5 amount effectively incorporated was 0.63 and 1.25 mol % respectively. Considering the fact that zircon was the preferential crystallised phase in the P_2O_5 glasses, we can assume that the incorporated P_2O_5 in the GCZP15 glass was not enough to produce a high volume fraction of crystals. This allows us to deduce that zircon crystals were grown from a low number of nuclei throughout a higher amount of residual glass phase, which leads to higher densification by viscous flow. These considerations also can be used to justify the higher densification of GCZP30 glass with respect to GCZ glass, since in this case, it seems by comparing micrographs of Fig. 11a, b and c that the volume fraction of crystals is higher in the glass composition GCZ and lower in the glass composition GCZP15 and GCZP30 in agreement with the crystallinity data. This happens because lithium disilicate crystallisation also competes with zircon crystallisation.

4. Conclusions

Lithium disilicate-zircon-based glass-ceramics containing 0.63 and 1.25 mol % of P_2O_5 were produced by sintering and crystallisation of a suitable glass powder in the Li_2O-ZrO_2-SiO_2 system having a base composition of 11.5 wt % Li_2O, 22.8 wt % ZrO_2, 65.7 wt % SiO_2.

Sintering was found to start at about 650°C and was completed in a very short temperature interval ($\Delta T \approx 100$°C) and a heating time lower than 30 min. Crystallisation took place just after densification and was almost completed at about 900°C for a heating time of about 20 min. A decrease in the sintered density as a consequence of secondary porosity which can be explained by considering both the viscosity and the crystallisation tendency of the parent glasses, was detected and evidenced during crystallisation stage. On heating, the glass powder compacts first crystallised into lithium metasilicate (Li_2SiO_3) and/or zircon ($ZrSiO_4$) and tridymite (SiO_2) which transformed and/or growth into lithium disilicate ($Li_2Si_2O_5$), zircon and tridymite after the crystallisation process was essentially complete. P_2O_5 doping little affected the densification of 11.5 wt % Li_2O, 22.8 wt % ZrO_2, 65.7 wt % SiO_2 glass powder. However, adding P_2O_5 remarkably enhanced zircon and tridymite crystallisation while delaying the lithium metasilicate and lithium disilicate transformations. The microstructure in general consists of fine crystals uniformly distributed and arbitrarily oriented throughout the residual glassy phase as well as a secondary porosity over the primary porosity.

Acknowledgement

Support for A. P. Novaes de Oliveira was provided by the "Fundação Coordenação de Aperfeiçoamento de Pessoal de Nível Superior - CAPES" and by Federal University of Santa Catarina, both Brazilian institutions. Additional support for the authors was provided by MURST.

References

1. Z. STRNAD, "Glass Science and Technology 8" (Elsevier, New York, 1986) p. 9.
2. E. M. RABINOVICH, *J. Mater. Sci.* **20** (1985) 4259.
3. M. H. LEWIS, "Glasses and Glass-Ceramics" (Chapman and Hall, London, 1989) p. 246, 88.
4. P. R. CARPENTER, M. CAMPBELL, R. D. RAWLINGS and P. S. ROGERS, *J. Mater. Sci. Lett.* **5** (1986) 1309.
5. J.-J. SHYN and H.-H. LEE, *J. Amer. Ceram. Soc.* **78**(8) (1995) 2161.
6. F. H. CHUNG, *J. Appl. Cryst.* **7** (1974) 519.
7. R. M. GERMAN, "Engineered Materials Handbook," Vol. 4, Ceramic and Glasses (ASM International, Metals Park, OH, 1991) p. 263.
8. M. F. Yan, "Engineered Materials Handbook," Vol. 4, Ceramic and Glasses (ASM International, Metals Park, OH, 1991) p. 273.
9. M. I. BUDD, *J. Mater. Sci.*, **28** (1993) 1007.
10. E. M. RABINOVICH, in "Advances in Ceramics," Vol. 4, Nucleation and Crystallisation in Glasses, edited by J. H. Simmons, D. R. Uhlmann and G. H. Beall (American Ceramic Society, Columbus, Ohio, 1982) p. 327.
11. A. P. NOVAES DE OLIVEIRA, A. B. CORRADI, L. BARBIERI, C. LEONELLI and T. MANFREDINI, *Thermochimica Acta* 2968 (1996) 1.
12. P. F. JAMES, in "Advances in Ceramics," vol. 4, Nucleation and Crystallisation in Glasses, edited by J. H. Simmons, D. R. Uhlmann and G. H. Beall (American Ceramic Society, Columbus, Ohio, 1982) p. 1.

Received 26 February 1998
and accepted 8 November 2000